iJRASET
International Journal For Research in Applied Science and Engineering Technology

INTERNATIONAL JOURNAL FOR RESEARCH

IN APPLIED SCIENCE & ENGINEERING TECHNOLOGY

Volume: 11 **Issue:** V **Month of publication:** May 2023

DOI: https://doi.org/10.22214/ijraset.2023.51717

www.ijraset.com

Call: 08813907089 | E-mail ID: ijraset@gmail.com

International Journal for Research in Applied Science & Engineering Technology (IJRASET)
ISSN: 2321-9653; IC Value: 45.98; SJ Impact Factor: 7.538
Volume 11 Issue V May 2023- Available at www.ijraset.com

Comparison of Signal Processing Methods for Bearing Fault Detection

Jitendra A. Gaikwad[1], Sanika S. Patankar[2], Prithiviraj Kamalapure[3], Prasad Patil[4], Tejas Kamble[5], Sumit Padole[6], Naseer Lahwal[7]

[1, 2, 3, 4, 5, 6, 7]*Department of Instrumentation Engineering Vishwakarma Institute of Technology Pune, Maharashtra, India 411037*

Abstract: ***Bearings with rolling elements are a typical part of rotating machinery. Vibration analysis is one of them that is frequently used to gauge the general wellbeing and condition of rotating machinery. Finding bearing defects is important in the pursuit of extremely reliable operations. The main relationship between vibration signal-based features and measured signals is that they can be used in order to assess the condition of a bearing. In order to examine the effectiveness of non-parametric harmonic approaches for defect identification using real motor data, the study recommends utilizing Thomson's Multitaper Estimation and Welch Periodogram Estimation. The researches show that this approach can identify outer race faults and inner race fault. The conclusive evidence points to Thomson's Multitaper Periodogram Estimation method as a successful technique for bearing fault identification.***

Keywords: Thomson's Multitaper Periodogram, Welch Periodogram, Condition Monitoring, Vibration, Bearing Failure Detection;

I. INTRODUCTION

Rotating machines have significant applications in our day to day lives. The state of the rotating machines should be monitored using various maintenance techniques for prediction and prevention. Any component, such as the stator, rotor, gear, and bearing, of a spinning machine may have flaws. Because of their straightforward design and high level of dependability, bearings are an essential and core component of all spinning equipment. According to the findings of numerous studies, bearing issues account for between 40 and 50 percent of all machine failures, which could further result in harmful machine breakdowns. The failure of bearing is expensive, yet it is a fundamental cause of lean system failure. Monitoring machine parameters to detect the emergence of a malfunction is known as condition monitoring (CM). The study suggests employing Welch Periodogram Estimation and Thomson's Multitaper Estimation to investigate the efficacy of non-parametric harmonic techniques for fault diagnosis using real motor data. Studies reveal that this method may recognize both inner and exterior racial problems. The indisputable evidence supports Thomson's Multitaper Periodogram Estimation method as an effective tool for identifying bearing faults.

II. METHODS AND MATERIALS

A. Experimental Setup

The design of the test rig to conduct research on rolling element bearings is introduced in this chapter. With the help of this proof-of-concept test equipment, spinning roller bearings with and without defects can be subjected to a variety of light radial and axial loads in order to establish a correlation for the fault growths on a bearing. This section describes how an experiment is conducted and how the results are compared to theoretical values.

Fig.1. Experimental Setup

Experimental investigation involves creating a mechanical design for the experimental setup and using that setup to analyses vibration signals and find bearing defects. The experimental setup includes a PMDC motor, a speed regulator, a load, a vibration measuring sensor, a Data Acquisition Card (DAQ), and ultimately a computer for data analysis using MATLAB software.

The vibration signal from the motor's front bearing is recorded using NI 9234. Welch's periodogram estimate and the classical periodogram are both used to analyses the received signal. In MATLAB software, the entire analysis and classification of defects is carried out. The 0.25 HP PMDC motor utilized in this study's experimental setup rotates a 1 kg load at 1000 revolutions per minute. Regulator changes the speed of the motor. The bearing is housed inside a bearing case on the shaft at the front of the motor. Three types of bearing conditions—normal bearing condition, outer race defect, and inner race defect—are explored here by changing the roller bearing in the electric motor [5]. As a test bearing, SKF 6203 2RS bearing is utilized. The table below shows the fundamental dimensions of the test bearing.

Bearing -	Pitch Diameter *Pd* (mm)	Ball Diameter *Bd* (mm)	Number of balls *Nb*	Angle of Contact θ(degrees)
SKF 6203 2RS	28.7	6.747	8	0

Table1: Test Bearing Dimensions

B. Bearing Characteristics fault frequencies

As shown in Figure 2, the majority of the bearing is composed of the outer racial flaw, inner racial deficiency, balls flaw, and cage flaw that ensures equal spacing between the balls [1].

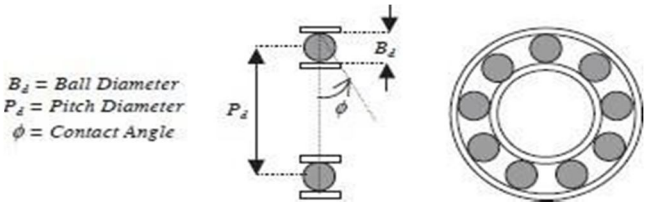

Fig.2. Ball Bearing construction Based on the component that is affected, there are four main types of bearing problems that can develop in bearings: ▪ Outer-race flaw

1) Inner racial deficiency
2) Cage flaw
3) Ball flaw

A certain amount of vibration occurs in every healthy bearing. An obtained acceleration signal can be used to identify whether there are any bearing defects or not. The magnitudes of the various vibrational components in the signal vary. The vibration signal is influenced by the bearing arrangement, number of rolling components, rotational speed, defect location, and type of applied load. Finding problems with the bearings of important machinery at an early stage of a problem is a terrific thing in an advanced industry. Inner racial deficiency, outer-race flaw, and rolling portion failures for a bearing configuration provide vibration signals with unique frequency components. The bearing's condition is determined by specific frequency components and their magnitudes. Bearing defect frequencies and motor speed are inversely correlated with one another. To determine characteristic fault frequencies, use the following equations:

$$f0 = \frac{Nb}{2} fr\left(1 - \frac{db\cos(\beta)}{dp}\right) \quad for\ BOF$$

$$fi = \frac{Nb}{2} fr\left(1 + \frac{db\cos(\beta)}{dp}\right) \quad for\ BIF$$

$$fb = \frac{dp}{db} fr\left(1 - \left(\frac{db\cos(\beta)}{dp}\right)^2\right) \quad for\ BBF$$

Where BOF, BIF and BBF indicate three types of ball bearing faults as outer-racial flaw, inner-racial flaw and ball bearing fault respectively. Nb is number of balls present in the bearing, and fb is the frequency of the ball fault. dp is the diameter of the pitch ball (with the races). The defect frequency can be estimated using bearing geometry and its speed as bearing has a unique rotational fault frequency depending on its kinematics [1]. It is possible to notice a change in the vibration levels at this frequency if a specific problem is forced on a bearing element [9].

C. Welch Periodogram

The periodogram approach, which is based on DFT, is a technique for estimating power spectrum. A continuous time signal, x(t), is sampled to create a discrete time signal, x[n], where nT is the sampling interval. The discrete time Fourier transform (DTFT) of the autocorrelation function of rxx[k], x[n], and x[n] can be used to calculate the power spectral density of x[n] at frequency f in accordance with the WienerKhintchine theorem [3].

$$P_{xx}(f) = T\sum_{k=8} x[k]e^{-j2\pi f k T}$$

In this Welch Periodogram method of spectrum analysis on bearing defect identification is presented. The motor data for this investigation was acquired in a real experiment setting in a lab setting. For various motor load circumstances, the researched spectrum method's failure detection has been tested. The spectrum amplitudes of sound and damaged motor data are contrasted for the Welch's Periodogram technique.

The first K segments of the data sequence [n], x [0], x [1] ..., x [N 1] are divided into by Welch's Periodogram method. With (L-S) overlapping samples, where S is the number of points to shift between segments, each segment [3], which has a length of L samples, can overlap another.

Segment 1: [0], [1], … , $x[L - 1]$ Segment 2: $[S]$, $[S + 1],\ldots,x[L+S-1]$

Segment K: $[N - L]$, $[N - L + 1],\ldots,x[N-1]$.

$x^{k}[n] = [n][n + kS]$ for $0 \le n \le L - 1$

$0 \le k \le K - 1$

w[n] is the window function that was applied to the data at each segment before to computing the segment periodogram [3]. Across the frequency range $-1/2T \le f \le 1/2T$ as, the weighted segment's sample spectrum is shown [3].

$$P_{xx}(f) = \frac{1}{ULT} X^{p}[X^{p}(f)]^{*} = \frac{1}{ULT} |X_{p}(f)|2$$

$$U = T\sum_{n=0}^{L-1} w^{(2)}[n]$$

$$X_{p}(f) = T\sum_{n=0}^{L-1} x_{(k)}[n]e^{-2\pi j f n T}$$

Where U denotes the energy of a discrete time window, and Xp(f) stands for the DTFT of the kth segment [4]. Simply take the periodogram values for the K segments and average them to obtain an estimate of the Welch's PSD [4].

$$\hat{P_{W}}(f) = \frac{1}{K}\sum_{k=0}^{K-1} \hat{P}(f)_{x} x(f)$$

D. Thomson's Multitaper Estimation

Multitaper denotes the use of multiple tapers (windows) to determine the signal estimate. Using an average of the number of independent spectrum estimators, the multitaper technique of spectrum estimating controls the variation in change. To detect leakage of the direct spectrum estimator, these estimators are nothing more than discrete prolate spheroidal sequence.

As long as x(n) is a stationary discrete-time random process with real values, it is possible. The process's spectrum Sx(f) must be estimated using the estimator from N samples of the process, X=. K

1

$$S\hat{}x = \_\sum S\hat{}k\ (f)$$

$k\ k = 1$

where,

$$S\hat{}(f) = |\sum\ (n)hk(n)e^{-i2\pi fn}|^2$$

$n = 0$

The windowed periodogram in Equation (2) was created by employing the data = [hk (0) ...hk(N-1)] T. The Multitaper estimate in Eq. is obtained by averaging K periodograms.

In multitaper periodogram white noise is removed using bank of FIR filters with fixed bandwidth. The associated frequency functions are and the impulse signal of the sub filters is hk [1].

$$H\ k\ (f) = hk^{T}.\emptyset(f)$$

Where,

$$(f\ ) = [1e^{-i2\pi f}\ \ldots\ e^{-i2(N-1)f}\ ]^2$$

The white noise spectrum is

$$(f\ )\ = 1$$

Given the input signal x, the output signal's strength inside the frequency range (-B/2; B/2) equals (n)[1],

$$P\ B\ = \int_{-B/2}^{B/2} |(f)|^2\ S\ w\ (f)\,df$$

$$= \int_{-B/2}^{B/2} \emptyset(f) Sw(f) \emptyset^{H}(f) df\ hk^{T} k$$

$$= hk \int_{-1}^{1} \emptyset(f)\ S\ w\ (f)\ \emptyset^{H}\ (f)\,d\ f\ \mathrm{h}k$$

$$= \mathrm{h}k^{T}\ \mathrm{R}B\ \mathrm{hk}$$

The components of the Toeplitz (NN) covariance matrix RB are

$$(l) = \int_{-\infty}^{\infty} SB(f)e^{-i2}\ r\ B^{\pi lf}\ d\ f = B\ \sin c\ (\pi\ B\ l\ )$$

$$0\ \leq |l\ | \leq N\ -\ 1, \text{ where } \operatorname{sinc}(x) = \frac{\sin(x)}{x}.$$

The optimization is carried out under the condition that the total power of a window equals one [1], or in other words, Multitaper makes use of the KT window's hk feature to maximise PB.

$$\text{Ptot} = \int_{-1}^{1} \lceil (f)|^2\ d = hk^{T}\ hk = 1$$

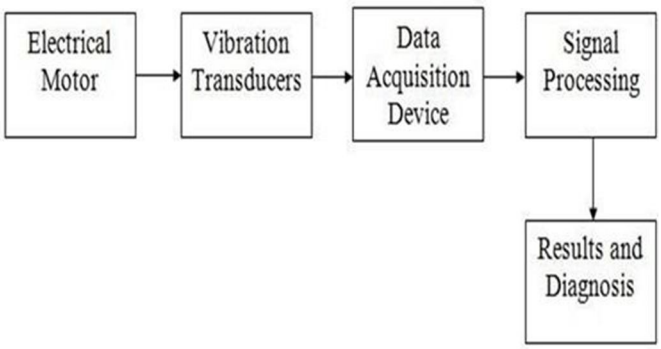

Fig.3. Block Diagram

III. METHODOLOGY

Figure 3 shows block diagram of the experimentation. The details of the same are as given below

1) Connect the MATLAB to NI 9234 device for taking the vibration signals generated from bearings.
2) Mount the vibration sensor on the PMDC motor and connect it to the NI 9234 device for taking the readings.
3) First take the readings of the different size of the loads i.e., 1kg, 2kg and 3kg at the different speeds i.e., 500, 1000 and 1500rpm by adjusting speed on the regulator.
4) Then take the readings of bearings i.e., Normal, Outer race and inner race bearings at the different speeds i.e., 500, 1000 and 1500rpm by adjusting speed on the regulator.
5) Use the data acquisition software from National Instruments to collect the data simultaneously.
6) Get the data into the MATLAB environment for postprocessing and evaluate the signals using the approach of your choice.
7) These readings will be generated in the excel sheets so save these according to their names.
8) These generated signals will be in time domain so convert these signals into frequency domain i.e., FFT.
9) After this apply Welch's Periodogram algorithm for more accuracy of the faulty bearings.
10) Compare theoretical characteristic frequency with practical results for faulty bearing.

IV. EXPERIMENTATION AND RESULTS

Table 2 below displays the fault details of the outer race flaw, inner racial deficiency, and healthy for the PMDC motor at different speeds of 500, 1000, and 1500 rpm. Theoretically estimated bearing defect frequencies for the outer and inner races are 50.99 Hz and 82.33 Hz, respectively, whereas the frequencies for healthy bearings are 16.66 Hz.

Table2: Frequencies of Bearing Fault At Different Speed

Speed	Actual Value	Estimation Value (Welch Periodogram)	Estimation Value (Thomson Multitaper)
Outer Race Fault			
500rpm	50.99	45.89	48.63
1000rpm	50.99	48.82	50.29
1500rpm	50.99	49.80	51.06
Inner Race Fault			
500rpm	82.33	81.05	87.53
1000rpm	82.33	78.12	83.00
1500rpm	82.33	79.58	78.12
Normal Bearing			
500rpm	16.66	15.62	17.02
1000rpm	16.66	19.53	16.11
1500rpm	16.66	16.60	16.53

Table 3 shows the raceways and bearing defects cause vibrations to occur at specific frequencies for a specific bearing geometry. The typical average frequencies of faulty bearings are determined as follows for both estimations: -

$$\% \text{ Error} = \frac{\text{Actual value} - \text{Estimated value}}{\text{Actual value}}$$

Table 3: Performance Comparison

Bearing Fault type	% Error (Welch Periodogram)	% Error (Thomson Multitaper
Outer Race Fault	5.5%	2%
Inner Race Fault	3.3%	0.7%
Normal Bearing	3.5%	0.6%

1) Result for outer race at 500rpm

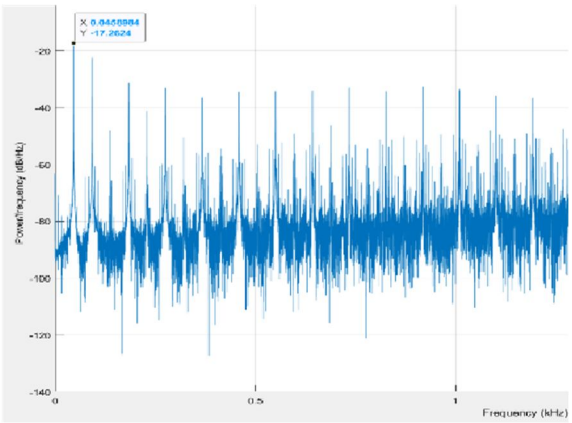

Fig(a). Welch periodogram for outer race fault(500rpm)

2) Result for outer race at 1000rpm

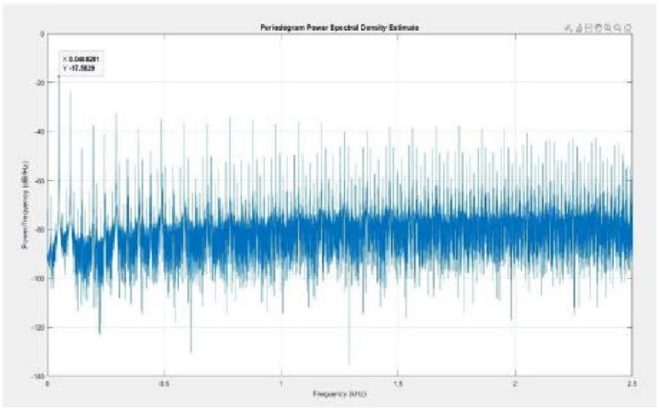

Fig(b). Welch Periodogram for outer race fault(1000rpm)

3) Result for outer race at 1500rpm

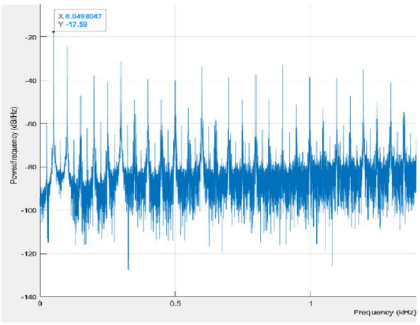

Fig(c). Welch periodogram for outer race fault(1500rpm)

4) Result for inner race at 500rpm

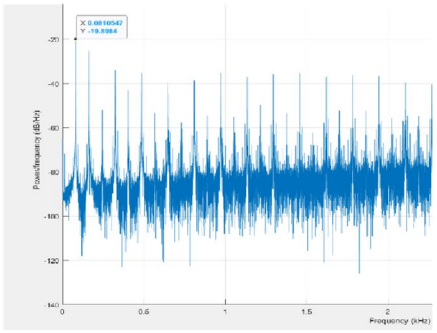

Fig(d). Welch periodogram for inner race fault(500rpm)

5) Result for inner race at 1000rpm

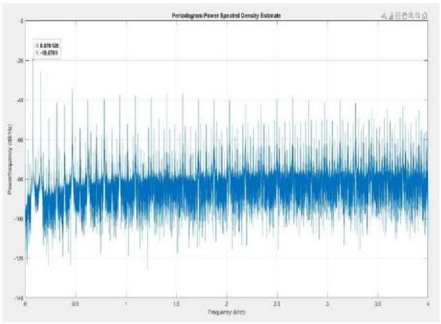

Fig(e). Welch periodogram for inner race fault(1000rpm)

6) Result for inner race at 1500rpm

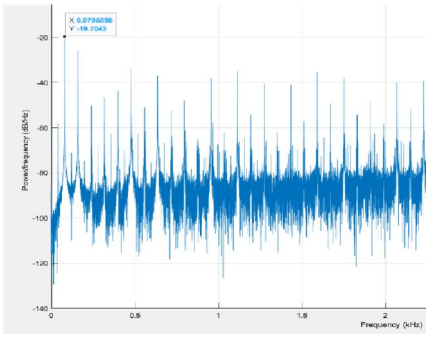

Fig(f). Welch periodogram for inner race fault(1500rpm)

7) Result for normal bearing at 500rpm

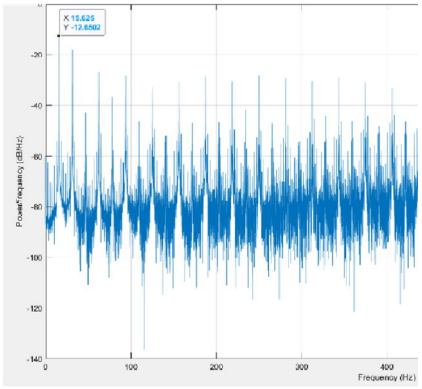

Fig(g). Welch periodogram for normal bearing(500rpm)

8) Result for normal bearing at 1000rpm

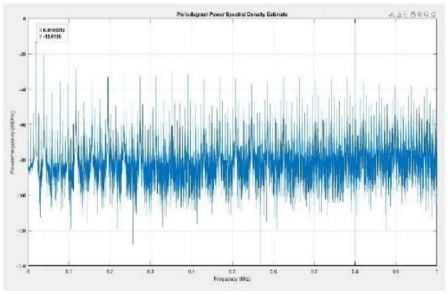

Fig(h). Welch periodogram for normal bearing(1000rpm)

9) Result for normal bearing at 1500rpm

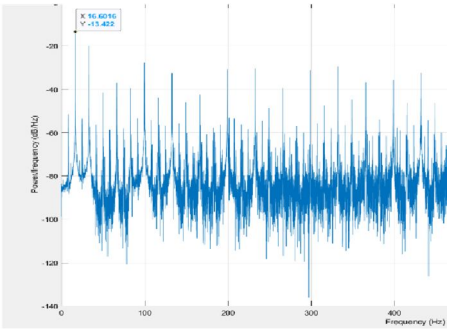

Fig(i). Welch periodogram for normal bearing(1500rpm)

10) Result for outer race at 500rpm

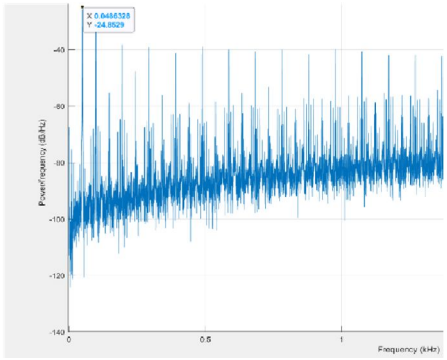

Fig(j). Thomson multitaper for outer race fault(500rpm)

11) Result for outer race at 1000rpm

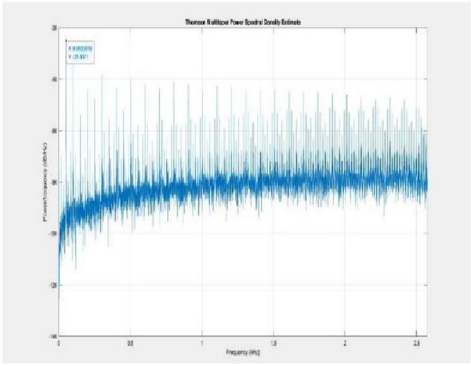

Fig(k). Thomson multitaper for outer race fault(1000rpm)

12) Result for outer race at 1500rpm

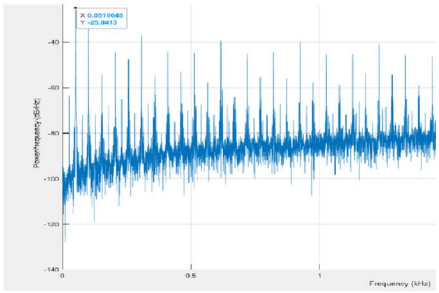

Fig(l). Thomson multitaper for outer race fault(1500rpm)

13) Result for inner race at 500rpm

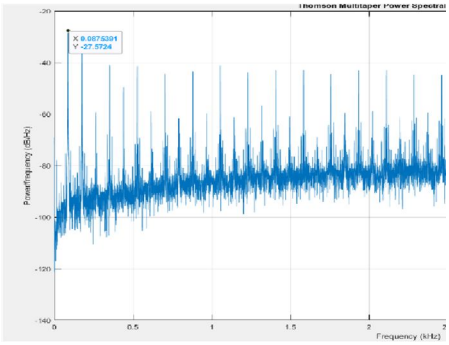

Fig(m). Thomson multitaper for inner race fault(500rpm)

14) Result for inner race at 1000rpm

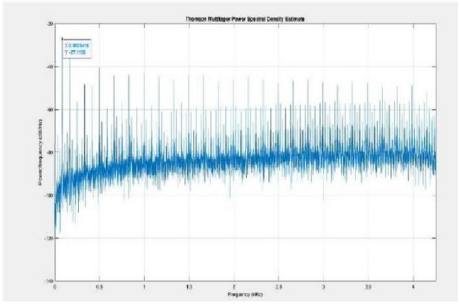

Fig(n). Thomson multitaper for inner race fault(1000rpm)

15) Result for inner at 1500rpm

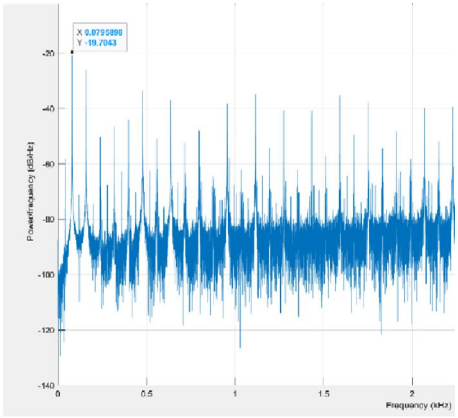

Fig(n). Thomson multitaper for inner race fault(1500rpm)

16) Result for normal bearing at 500rpm

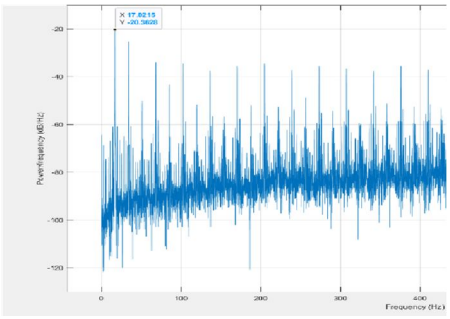

Fig(o). Thomson multitaper for normal bearing(500rpm)

17) Result for normal bearing at 1000rpm

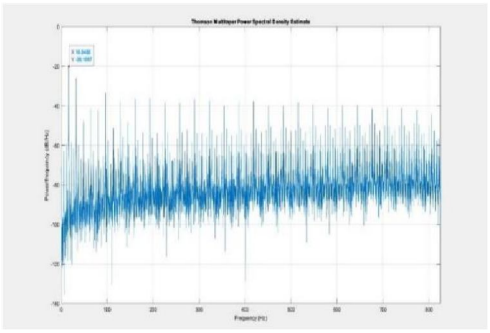

Fig(p). Thomson multitaper for normal bearing(1000rpm)

18) Result for normal bearing at 1500rpm

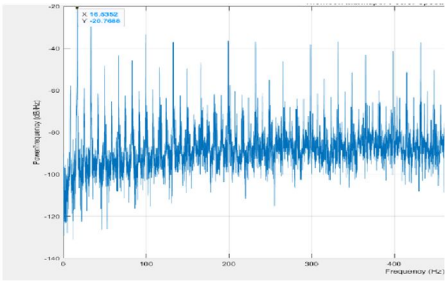

Fig(q). Thomson multitaper for normal bearing(1500rpm)

V. FUTURE SCOPE

Develop different detection methods for better fault detection. Study different responsible parameters like air gap eccentricity, stator and rotor conditions for development of fault in bearing and motor. We will apply more different algorithms like Gaussian filter, Wavelet, for more better accuracy of outer racial flaw and inner racial flaw bearing.

VI. CONCLUSION

For the detection of bearing outer race flaw and inner racial deficiency faults, Welch Periodogram and Thomson's Multitaper Estimation are utilized [11]. The theoretical and practical values of the defect frequency for outer race and inner race are very similar. According to the findings based on experimental motor data, the Thomson's Multitaper approach exhibits greater discrimination capabilities when compared to the fundamental Welch periodogram method. Additionally, it makes it abundantly evident how much more reliable the Thomson's Multitaper Periodogram approach is than the fundamental Welch periodogram method. Averaging Thomson's Multitaper estimate technique provides in accurate, smooth, and less noisy output by efficiently reducing the variance of the periodogram.

REFERENCES

[1] Jitendra A. Gaikwad, Yogesh B. Gholap, Jayant V. Kulkarni. "Bearing Fault Detection Using Thomson's Multitaper Periodogram", 2018 Second International Conference on Intelligent Computing and Control Systems (ICICCS), 2018
[2] D. Thomson," Spectrum estimation and harmonic analysis"Proc.of the IEEE,vol.70,no.9,pp.10551096,sept 1982.
[3] B. Ayhan, Mo-Yuen Chow, H.J. Trussell, Myung-Hyun Song. "A case study on the comparison of nonparametric spectrum methods for broken rotor bar fault detection", IECON'03. 29th Annual Conference of the IEEE Industrial Electronics Society (IEEE Cat. No.03CH37468), 2003
[4] Reshma Kunjir, Vijaykumar Bhanuse, Jayant Kulkarni, Sanika Patankar. "Determination of Deformation of Steel Plate Using Welch's Periodogram Estimate", 2018 Second International Conference on Intelligent Computing and Control Systems (ICICCS), 2018A. T. Walden, "A unified view of multitaper multivariate spectral estimation," Biometrika, vol. 87, no. 4, pp. 767– 788, 2000.
[5] Smita A. Chopade, Jitendra A. Gaikwad, Jayant V. Kulkarni. "Bearing fault detection using PCA and Wavelet based envelope analysis", 2016 2nd International 278 words — 10% 115 words — 4% 47 words — 2% 33 words — 1% 22 words — 1% 6 7 8 9 10 11 12 13 Conference on Applied and Theoretical Computing and Communication Technology (iCATccT), 2016
[6] D. M. Yang, "Induction motor bearing fault detection using wavelet-based envelope analysis", International Symposium on Computer, Consumer and Control, pp.1241-1244, 2014.
[7] Bostjan Dolenc and Pavle Baskoski,''Distributed Bearing fault diagnosis Based on vibration analysis'', Elsevier ,mechanical systems and signal Processing ,vol.66-67pp.521-532,jan 2016.
[8] Mehmat Ali and Selahattin Guclu ,"Vibration analysis of induction motors with unbalanced loads"; Ebeoglu.pp.365- 369.10th International Conference on Electrical and Electronics Engineering (ELECO), 2017.
[9] Bujoreanu, Carmen, and Florin Breabăn. "Bearing Scuffing Detection and Condition Monitoring Using Virtual Instrumentation", Applied Mechanics and Materials, 2014.
[10] Maria Hansson-Sandsten, "A Welch Method approximation of the Thomson's Multitaper Spectrum Estimator",.20th European Signal processing Conference Aug 2012.
[11] Muhammad Amir Khan, Bilal Asad, Karolina Kudelina, Toomas Vaimann, Ants Kallaste. "The Bearing Faults Detection Methods for Electrical Machines—The State of the Art", Energies, 2022

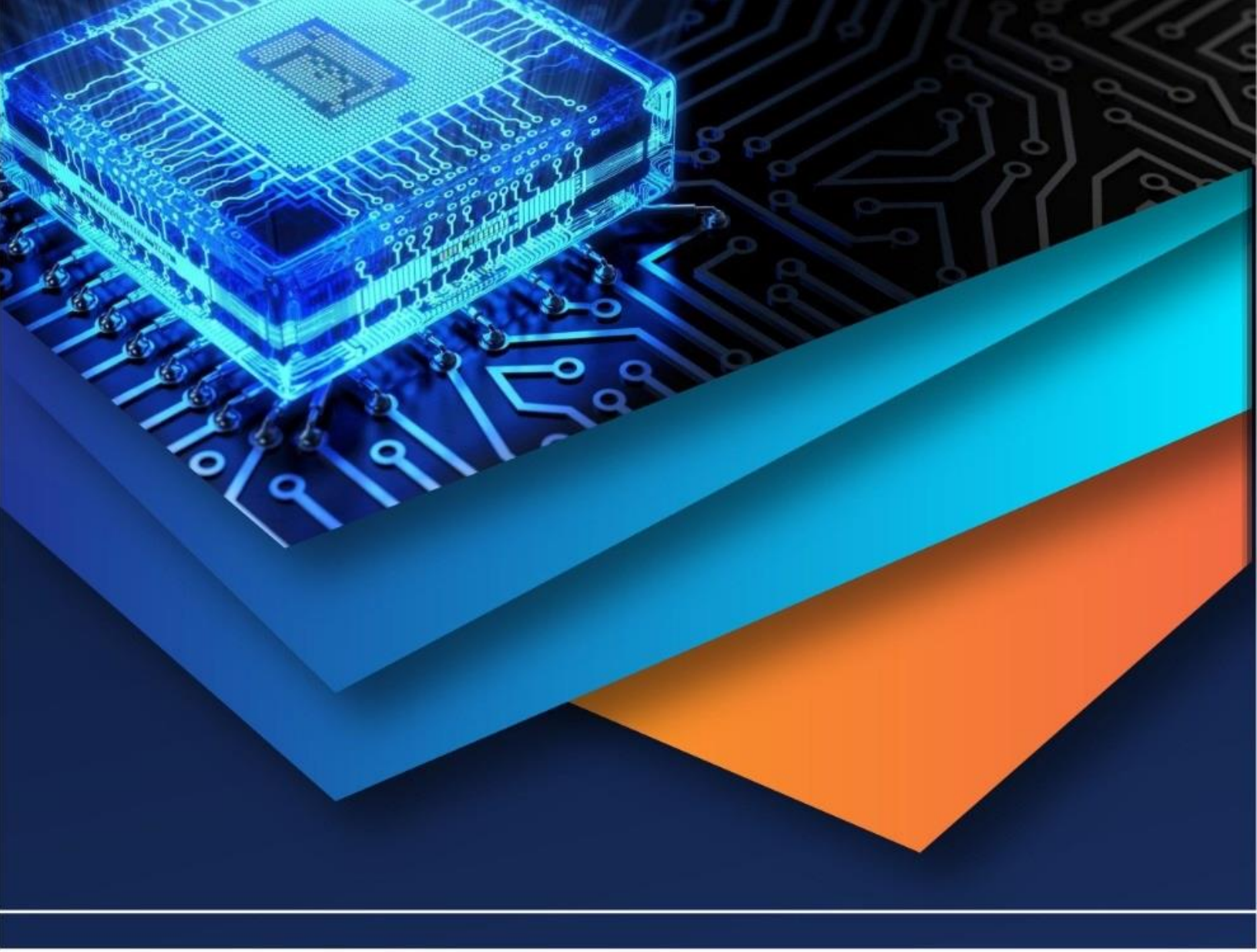

10.22214/IJRASET

45.98

IMPACT FACTOR: 7.129

IMPACT FACTOR: 7.429

INTERNATIONAL JOURNAL FOR RESEARCH

IN APPLIED SCIENCE & ENGINEERING TECHNOLOGY